

# Wavelet-Based Simulation of Spatially Correlated and Spectrum-Compatible Accelerograms

Kaushik Sarkar and Vinay K. Gupta

---

---

## ABSTRACT

*For the time-history analysis of a complex or non-linear extended structure under seismic excitation, it is useful to generate a set of properly correlated earthquake accelerograms that are consistent with a given (design) response spectrum and coherency structure. This paper describes a wavelet-based procedure to simulate ensembles of such accelerograms by replicating temporal variations in the frequency content of a (parent) recorded accelerogram. The procedure is based on an extension of the stochastic decomposition technique to wavelet domain while using the analytic form of the modified Littlewood-Paley (L-P) basis function.*

---

---

## INTRODUCTION

It is common to characterize seismic hazard at a site in terms of design (response) spectra. While those may be used directly for the linear analyses of single-degree-of-freedom and multi-degree-of-freedom systems, artificial time-histories of specified duration and compatibility with one such spectrum need to be generated for the seismic analyses of complex and non-linear structural systems. A method to be used for this purpose should account for the temporal variations in the frequency composition arising due to the arrivals of different types of seismic waves at different time-instants and due to the phenomenon of dispersion in these waves. Also, in case of spatially extended structures such as long span bridges, pipelines, possible variations in the earthquake ground motion at different points in space characterized usually by coherency function should be accounted for.

Though generation of spatially correlated accelerograms has been attempted by several researchers, most of the suggested procedures used a deterministic modulating function. This may disturb the coherency structure besides leading to unrealistic accelerograms due to 'too simplistic' modelling of the earthquake ground motion process. Shrikhande and Gupta<sup>[1]</sup> used the non-stationary characteristics of a given accelerogram via its phase and duration spectra, in the method of stochastic decomposition<sup>[2]</sup>, thus requiring no post-processing of the simulated motions and keeping the coherency structure

intact. Sarkar and Gupta<sup>[3]</sup> have recently improvised this approach by proposing a wavelet-based formulation, such that frequency non-stationarity is taken care of without putting any limitation on the target process to be used, and any recorded accelerogram can be used independent of the nature of the target response spectrum. Additionally, this formulation has the flexibility of including temporal variations in the correlation structure.

This paper describes the formulation of Sarkar and Gupta<sup>[3]</sup>. In this, the simulation is carried out through estimation of wavelet coefficients. These coefficients are obtained for the analytic equivalent of the modified L-P basis function<sup>[4]</sup>. The analytic form can decouple the amplitude and phase information of a signal, besides being able to decompose a signal into component time-histories having energy in non-overlapping frequency bands. For illustration, ensembles of accelerograms are generated at four stations 100, 200 and 300 m apart, corresponding to USNRC design spectrum and non-stationary characteristics of a 1978 Santa Barbara earthquake motion.

## SIMULATION PROCEDURE

The problem of simulation of spatially correlated time-histories is a multivariate simulation problem, as each of the ground motion records at different stations is basically a realization of the same event. Let  $F(t)$  denote the random multivariate process of spatially correlated time-histories at  $n$  stations. When  $F(t)$  is stationary, the spectral matrix for this process is defined as

$$S_F(\omega) = \begin{bmatrix} S_{11}(\omega) & S_{12}(\omega) & \dots & S_{1n}(\omega) \\ S_{21}(\omega) & S_{22}(\omega) & \dots & S_{2n}(\omega) \\ \vdots & \vdots & \ddots & \vdots \\ S_{n1}(\omega) & S_{n2}(\omega) & \dots & S_{nn}(\omega) \end{bmatrix} \quad (1)$$

where, the  $i$ th diagonal term denotes the power spectral density function (PSDF) of the  $i$ th element of  $F(t)$  (corresponding to the ground motion process at the  $i$ th station) and the  $(i, j)$ th off-diagonal term refers to the cross-PSDF between the  $i$ th and  $j$ th elements of  $F(t)$ . In order to consider the inherent non-stationarity in the seismic ground motions, the spectral matrix  $S_F(\omega)$  of the target process is estimated instantaneously in form of a series of instantaneous spectral matrices.

We first estimate the target instantaneous matrices through a wavelet-based characterization of  $F(t)$  and by the use of a suitable coherency function along with the spectrum-compatible instantaneous PSDFs. For a 'not too large' site, it may be assumed that the ground motions to be simulated at different stations conform to the same (specified) design spectra and thus, all diagonal elements of the (target) instantaneous matrices at any instant are identical. We also assume that a suitable (parent) accelerogram conforming to the local source and site conditions is available. This accelerogram is first modified so as to be compatible with one of the design spectrum (corresponding to the damping ratio of the structural system), and then instantaneous PSDFs are obtained from the wavelet coefficients of the generated accelerogram. For modification of the parent accelerogram, the procedure described in the Appendix is used. In this procedure, the temporal variations in different (non-overlapping) frequency bands remain undisturbed during the modification. The instantaneous PSDFs are obtained from the spectrum-compatible accelerogram  $X(t)$  as

$$S_X(\omega)_t = \frac{K}{a_j} E \left[ \left| W_\psi X(a_j, b_j) \right|^2 \right] \left| \hat{\psi}_{a_j, b_j}(\omega) \right|^2 \quad (2)$$

where  $W_\psi X(a_j, b_j)$  is the wavelet coefficient for  $X(t)$  at scale parameter,  $a_j = \sigma^j$  and shift parameter,  $b_j = (i-1)\Delta b$  with  $\sigma = 2^{\frac{1}{2}}$ , and  $\Delta b = 0.02s$  being the sampling time interval of the accelerogram.

The wavelet coefficient is expressed as

$$W_\psi X(a_j, b_j) = \frac{1}{\sqrt{a_j}} \int_{-\infty}^{\infty} X(t) \psi^* \left( \frac{t-b_j}{a_j} \right) dt \quad (3)$$

$$\text{with } K = \frac{1}{4\pi C_\psi} \left( \sigma - \frac{1}{\sigma} \right) \quad (4)$$

$$\text{and } C_\psi = \int_{-\infty}^{\infty} \frac{|\hat{\psi}(\omega)|^2}{|\omega|} d\omega \quad (5)$$

In Eq. (2),  $\omega_j$  is a frequency (between  $\pi/a_j$  and  $\sigma\pi/a_j$ ) corresponding to the  $j$ th scale parameter. Further,  $\hat{\psi}_{a_j, b_j}(\omega_j)$

is the Fourier transform of  $\psi_{a_j, b_j}(t) = \psi \left( \frac{t-b_j}{a_j} \right) / \sqrt{a_j}$

with reference to the mother wavelet defined as

$$\psi(t) = \frac{e^{i\sigma\pi t} - e^{i\pi t}}{i\pi\sqrt{\sigma-1}} \quad (6)$$

In Eq. (3),  $\psi^*(\cdot)$  is the complex conjugate of  $\psi(\cdot)$ . In Eq. (5),

$$\begin{aligned} \hat{\psi}(\omega) &= \frac{1}{\sqrt{2\pi}} \int_{-\infty}^{\infty} \psi(t) e^{-i\omega t} dt \\ &= \frac{2}{\sqrt{2(\sigma-1)\pi}}; \quad \pi \leq \omega \leq \sigma\pi \\ &= 0; \quad \text{otherwise} \end{aligned} \quad (7)$$

is the Fourier transform of  $\psi(t)$

In the absence of a number of realizations, the ensemble averaging in Eq. (2) can be carried out through smoothing of various PSDFs. To estimate the off-diagonal terms of the spectral matrix, say the instantaneous cross-PSDF  $S_{mn}(\omega, t)$  between the motions at stations  $m$  and  $n$ , the instantaneous PSDF is to be multiplied with the corresponding instantaneous coherency function,  $\gamma_{mn}(\omega, t)$ , defined as

$$\gamma_{mn}(\omega, t) = \frac{S_{mn}(\omega, t)}{\sqrt{S_m(\omega, t) S_n(\omega, t)}} \quad (8)$$

In the absence of a functional model for this function, a time-invariant model proposed by Harichandran and Vanmarcke<sup>[5]</sup> is used here to describe correlations at all time-instants. This function is therefore expressed as

$$\gamma_{mn}(\omega, t) = \rho(r_{mn}, f) \exp \left[ \frac{i\omega r_{mn}}{v_{app}} \right] \quad (9)$$

with

$$\begin{aligned} &\rho(r_{mn}, f) \\ &= A \exp \left[ -\frac{2r_{mn}}{\theta(f)} (1-A + \alpha A) \right] \\ &+ (1-A) \exp \left[ -\frac{2r_{mn}}{\theta(f)} (1-A + \alpha A) \right] \end{aligned} \quad (10)$$

Here,  $v_{app}$  is the apparent velocity of propagation of seismic waves at the site under consideration,  $f = \omega/2\pi$  is

the wave frequency in Hz, and  $r_{mn}$  is the distance between the stations  $m$  and  $n$ . Further,

$$\theta(f) = k \left[ 1 + \left( \frac{f}{f_0} \right)^b \right]^{-1/2} \quad (11)$$

represents the frequency-dependent spatial scale of fluctuations; and  $A$ ,  $\alpha$ ,  $k$ ,  $f_0$ , and  $b$  are the parameters estimated by the regression analyses of the recorded data. On Cholesky decomposition, the (target) instantaneous spectral matrix may be expressed

$$S_F(\omega)|_{t=b_i} = L(\omega)|_{t=b_i} \cdot L^H(\omega)|_{t=b_i} \quad (12)$$

where  $L(\omega)|_{t=b_i}$  denotes the (complex) lower triangular factor of the spectral matrix at time instant  $t=b_i$ , and  $L^H(\omega)|_{t=b_i}$  is the transpose of the complex conjugate of  $L(\omega)|_{t=b_i}$ . The  $(m, n)$ th element of the instantaneous spectral matrix is thus obtained in terms of Cholesky factors

$$S_{mn}(\omega_j)|_{t=b_i} = \sum_{r=1}^m L_{mr}(\omega_j)|_{t=b_i} \cdot L_{nr}^*(\omega_j)|_{t=b_i} \quad (13)$$

for  $m < n$ , where  $L_{mr}(\omega_j)|_{t=b_i}$  denotes the  $(m, r)$ th element of  $L(\omega)|_{t=b_i}$  (at a frequency  $\omega_j$  of the  $j$ th frequency band), and  $L_{nr}^*(\omega_j)|_{t=b_i}$  is the complex conjugate of the  $(n, r)$ th element of the same matrix.

Accelerograms conforming to the (target) instantaneous spectral matrices are simulated by extending the method of stochastic decomposition in wavelet domain. Decomposing each of the elements of the multivariate process  $F(t)$  into the constituent sub-processes, the  $m$ th element of  $F(t)$  may be expressed as

$$F_m(t) = \sum_{r=1}^m F_{mr}(t) \quad (14)$$

where,  $F_{mr}(t)$  is a realization of the  $r$ th sub-process at station  $m$ . On taking wavelet transform of both sides, Eq. (14) may be expressed as

$$W_\psi F_m(a_j, b_i) = \sum_{r=1}^m A_{mr}(a_j, b_i) e^{i(\phi_{mr}(a_j, b_i) + \alpha_r(a_j))} \quad (15)$$

where  $W_\psi F_m(a_j, b_i)$  is the wavelet coefficient of  $F_m(t)$ , and  $A_{mr}(a_j, b_i)$  and  $(\phi_{mr}(a_j, b_i) + \alpha_r(a_j))$  are respectively the amplitude and argument of the wavelet coefficient of  $F_{mr}(t)$  corresponding to the  $j$ th scale and  $i$ th instant. Here,  $\alpha_r(a_j)$  is a random phase angle, varying with the scale parameter  $j$  and being uniformly distributed over the range 0 and  $2\pi$ . Assuming that the random phase angles  $\alpha_r(a_j)$  and  $\alpha_s(a_j)$  are statistically independent for all  $r \neq s$ , deterministic quantities  $A_{mr}(a_j, b_i)$  and  $\phi_{mr}(a_j, b_i)$  may be

obtained from the Cholesky factors of the instantaneous spectral matrix of  $F(t)$  as

$$A_{mr}(a_j, b_i) = \sqrt{\frac{a_j}{K}} \frac{1}{|\Psi_{a_j, b_i}(\omega_j)|} \left| L_{mr}(\omega_j) \right|_{t=b_i} \quad (16)$$

and

$$\phi_{mr}(a_j, b_i) = \tan^{-1} \frac{\text{Im}(L_{mr}(\omega_j)|_{t=b_i})}{\text{Re}(L_{mr}(\omega_j)|_{t=b_i})} \quad (17)$$

where  $\text{Im}(\cdot)$  and  $\text{Re}(\cdot)$  respectively denote the imaginary and real parts of the complex element inside the parenthesis.

Once the wavelet coefficients of the constituting sub-processes of each of the elements are estimated, those are used in Eq. (15) along with the statistically independent random phase angles to generate the wavelet coefficients of the realizations of the individual elements of  $F(t)$ . These coefficients are then inverse-transformed to obtain the corresponding time-histories as

$$f(t) = \frac{K\Delta b}{a_j} \text{Re} \left[ \sum_i \sum_j W_\psi f(a_j, b_i) \Psi \left( \frac{t-b_i}{a_j} \right) \right] \quad (18)$$

A use of different sets of random phase angles leads to the generation of ensembles.

## NUMERICAL ILLUSTRATION

The proposed approach is illustrated by synthesizing accelerograms at four stations, 100 m apart, and having non-stationary characteristics of the recorded motion at Cachuma dam, Santa Barbara, California, USA during the 1978 Santa Barbara earthquake. This accelerogram is shown in Fig. 1. The target design spectrum is taken to be the 5 percent USNRC design spectrum of 0.25g peak ground acceleration. Fig. 2 shows the instantaneous PSDFs at three arbitrarily chosen instants for the example motion. The parameters of the coherency function are considered as:  $v_{app} = 2500$  m/sec,  $A = 0.736$ ,  $\alpha = 0.147$ ,  $k = 5210$ ,  $f_0^{app} = 1.09$ , and  $b = 2.78$ . At each of the four stations, an ensemble of 20 records is simulated. Fig. 3 shows synthesized accelerograms corresponding to  $r_{ij} = 0, 100, 200, \text{ and } 300$  m for Stations 1-4. It may be seen that the simulated time histories look very similar to the original motion (see Fig. 1) in terms of temporal development.

The 5 percent damping (ensemble-averaged) response spectra for the simulated motions at each station are compared with the target spectrum in Fig. 4. The response spectra corresponding to  $r_{ij} = 0$  appear to be in good agreement with the target spectrum, whereas for other stations, greater fluctuations are observed around the target spectrum as a manifestation of the interference of different wave components. Depending upon whether there is a destructive or constructive interference at a particular

time-period, the spectral ordinates are found to be lower or higher. The fluctuations are so prominent in Fig. 4 due to a low value of  $v_{app}$ , chosen intentionally to emphasize the effect of interference and wave propagation.

The coherencies have also been computed for each of the (six) pairs of stations at 4 and 9 sec by considering ensembles of 20 accelerograms each. Figs. 5-10 show the comparisons for their absolute values with the target coherence (see Eq. (11)). Figs. 5-7 are for the stations 100 m apart (stations 1 and 2, stations 2 and 3, stations 3 and 4); Figs. 8-9 are for the stations 200 m apart (stations 1 and 3, stations 2 and 4); and Fig. 10 is for the stations 300 m apart (stations 1 and 4). It may be observed that the computed coherencies are in very good agreement with the target coherencies.

## CONCLUSIONS

A new method to generate ensembles of spatially correlated accelerograms at a given number of stations has been described. Numerical illustrations for four stations 100 m apart in case of USNRC design spectrum and a 1978 Santa Barbara earthquake motion show that the simulated motions nicely preserve the non-stationary characteristics of the example process and the specified (time-invariant) coherency structure at different instants of time. Also, the

ensembles of generated motions at each of the stations are compatible with the target response spectrum in the mean sense. Though it is assumed that the same set of response spectra characterize the seismic hazard at all stations, the method can be easily used to simulate motions compatible with different response spectra at different stations.

## APPENDIX: MODIFICATION OF ACCELEROGRAM

The method of Mukherjee and Gupta<sup>[6]</sup> to modify a recorded accelerogram to match with a given response

spectrum is briefly described here. The main idea behind this method is to decompose a given earthquake accelerogram into sufficient number of time-histories having energy in non-overlapping frequency bands and then to scale those component time-histories iteratively for matching with a given response spectrum. The recorded accelerogram,  $f(t)$ , is thus decomposed into  $N$  number of time-histories, i.e.,

$$f(t) = \sum_{j=1}^N f_j(t) \quad (19)$$

where,  $f_j(t)$  is the  $j$ th time-history given as

$$f_j(t) = \frac{K\Delta b}{a_j} \sum_i W_{\nu} f(a_j, b_i) \psi\left(\frac{t-b_i}{a_j}\right) \quad (20)$$

and  $N$  is such that  $f_1(t), f_2(t), \dots, f_N(t)$  cover the entire frequency range of significant energy in  $f(t)$ .

The time-history,  $f_j(t)$ , is iteratively scaled as

$$f_j^{(n+1)}(t) = f_j^{(n)}(t) \frac{\int_{2a_j/\sigma}^{2a_j} [PSA(T)]_{\text{target}} dT}{\int_{2a_j/\sigma}^{2a_j} [PSA^{(n)}(T)]_{\text{calculated}} dT} \quad (21)$$

where,  $[PSA(T)]_{\text{target}}$  is the ordinate of target response spectrum at period  $T$ , and  $[PSA^{(n)}(T)]_{\text{calculated}}$  is the ordinate

of response spectrum calculated from  $f^{(n)}\left(= \sum_{j=1}^N f_j^{(n)}\right)$  at the same  $T$  after  $n$  iterations. The iterative process is continued for all  $N$  component time-histories till the error in the calculated response spectrum, as averaged over the chosen control time-periods, falls below a specified tolerance level.

## REFERENCES

1. M. Shrikhande and V.K. Gupta, "Synthesizing ensembles of spatially correlated accelerograms," ASCE Journal of Engineering Mechanics, Vol. 124, No. 11, 1998, pp. 1185-1192.
2. M. Shinozuka, "Simulation of multivariate and multidimensional random processes," Journal of the Acoustical Society of America, Vol. 49, 1971, pp. 357-367.
3. K. Sarkar and V.K. Gupta, "Wavelet-based generation of spatially correlated accelerograms," Earthquake Engineering and Structural Dynamics (under review).

4. B. Basu and V.K. Gupta, "Seismic response of SDOF systems by wavelet modelling of nonstationary processes," ASCE Journal of Engineering Mechanics, Vol. 124, No. 10, 1998, pp. 1142-1150.
5. R.S. Harichandran and E.H. Vanmarcke, "Stochastic variation of earthquake ground motion in space and time", ASCE Journal of Engineering Mechanics, Vol. 112, 1986, pp. 154-174.
6. S. Mukherjee and V.K. Gupta, "Wavelet-based generation of spectrum-compatible time-histories," Soil Dynamics and Earthquake Engineering, Vol. 22, 2002, pp. 799-804.

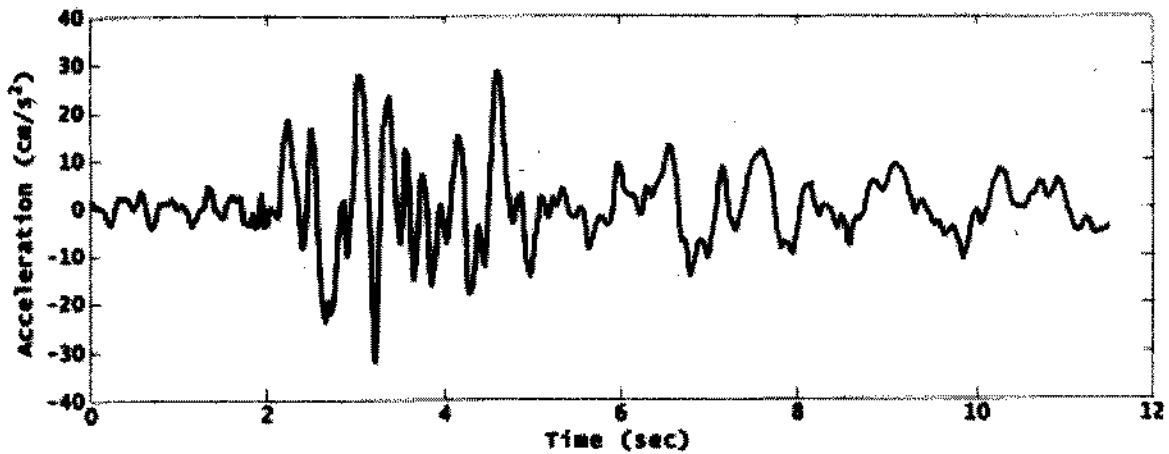


Fig. 1 Original (recorded) accelerogram for the example motion

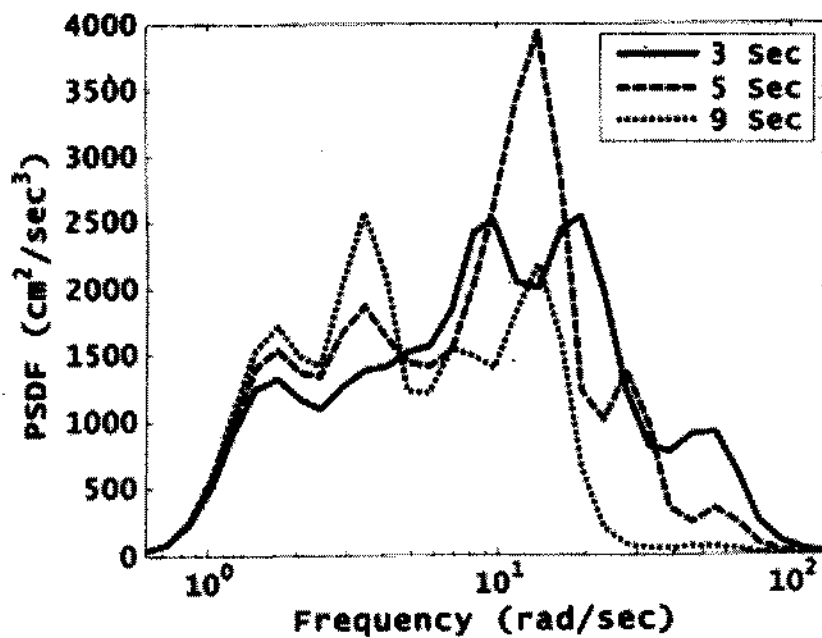


Fig. 2 Instantaneous PSDFs at different instants for the example motion

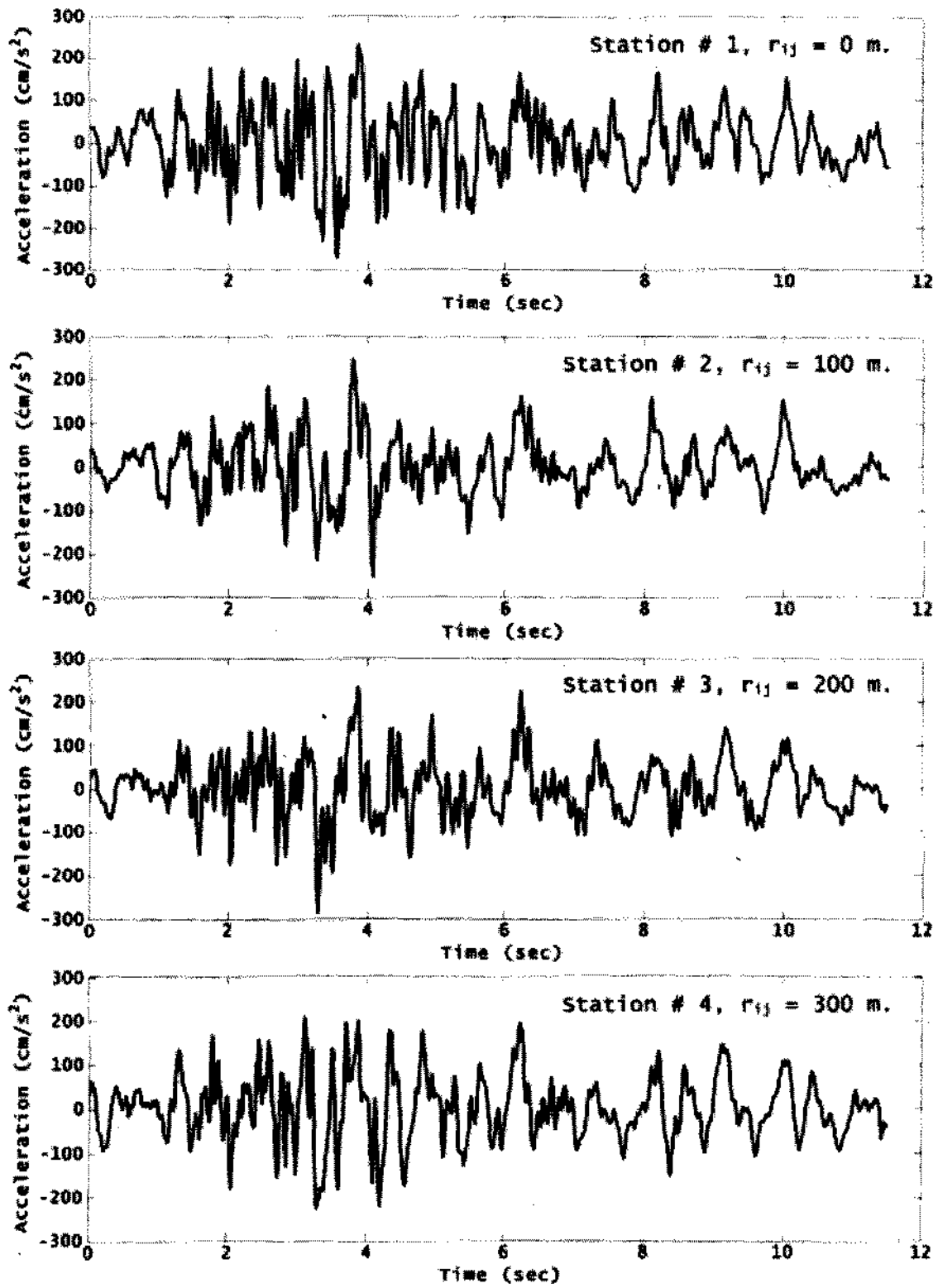


Fig. 3 Simulated ground motions at different stations with example motion characteristics

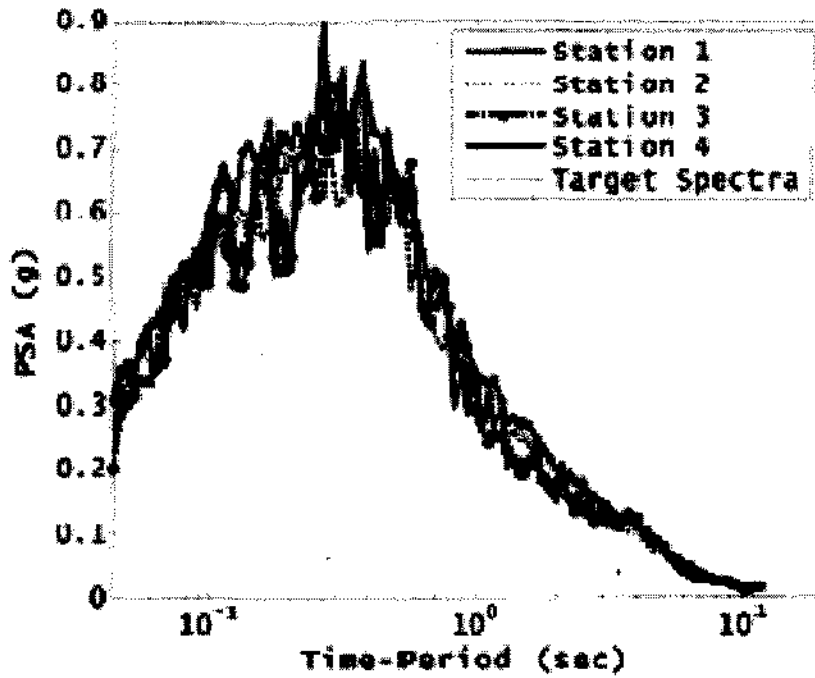


Fig. 4 Comparison of mean response spectra for ensembles of simulated accelerograms with example motion characteristics at different stations with the target spectrum

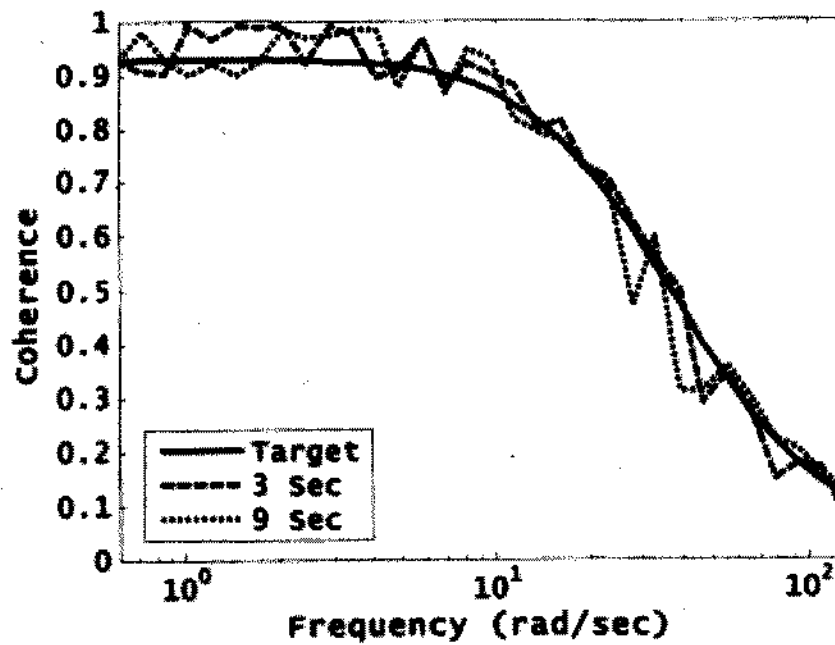


Fig. 5 Comparison of instantaneous coherences for the ensembles of accelerograms with example motion characteristics at stations 1 and 2 with the target coherence

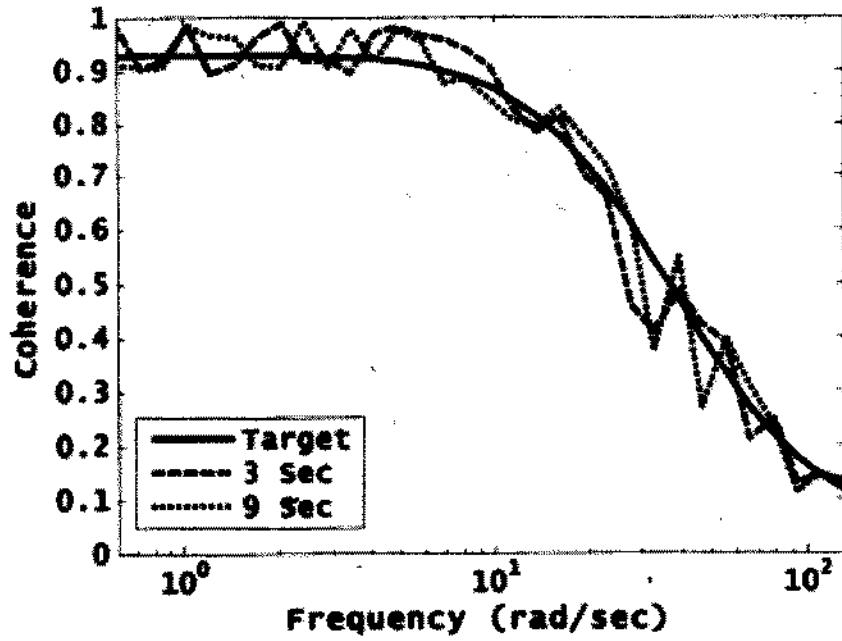


Fig. 6 Comparison of instantaneous coherences for the ensembles of accelerograms with example motion characteristics at stations 2 and 3 with the target coherence

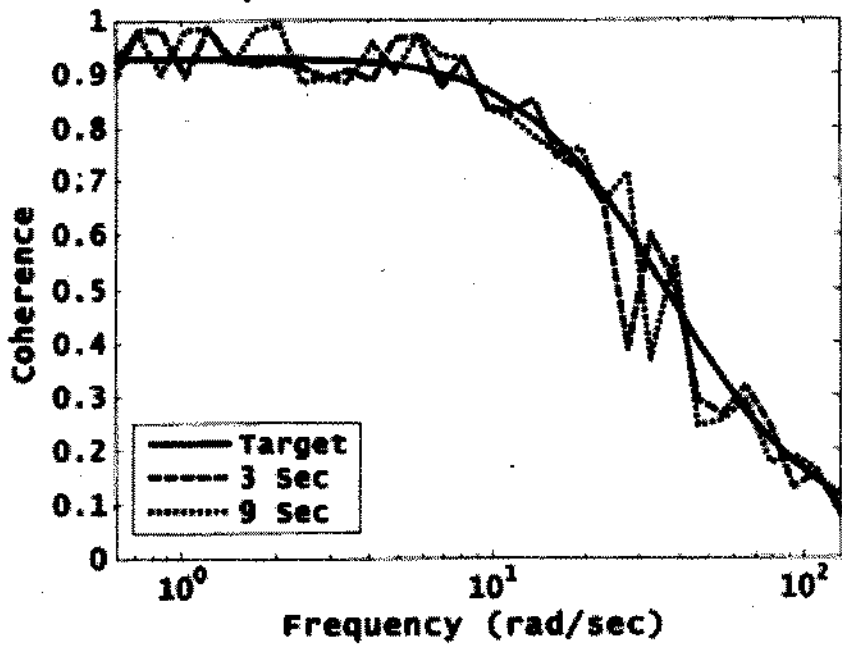


Fig. 7 Comparison of instantaneous coherences for the ensembles of accelerograms with example motion characteristics at stations 3 and 4 with the target coherence



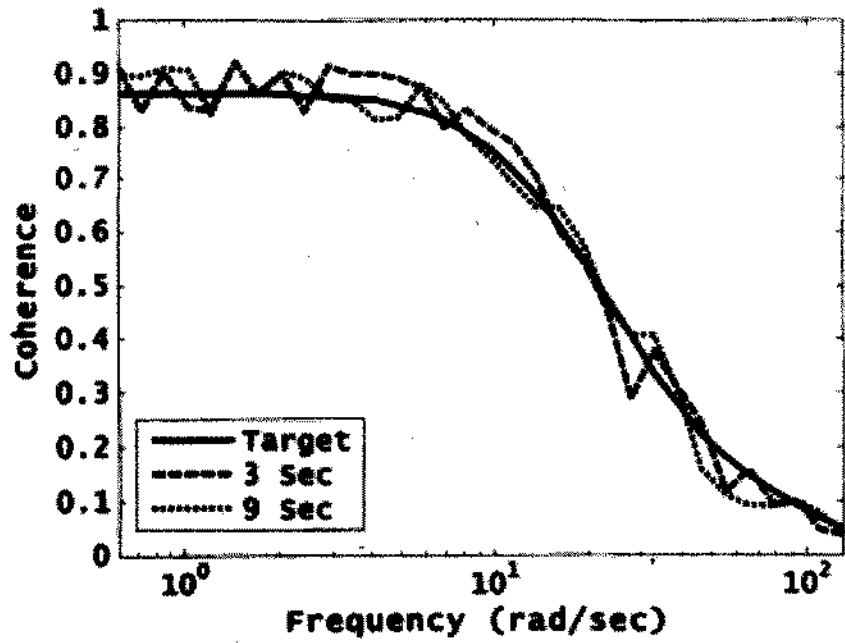


Fig. 8 Comparison of instantaneous coherences for the ensembles of accelerograms with example motion characteristics at stations 1 and 3 with the target coherence

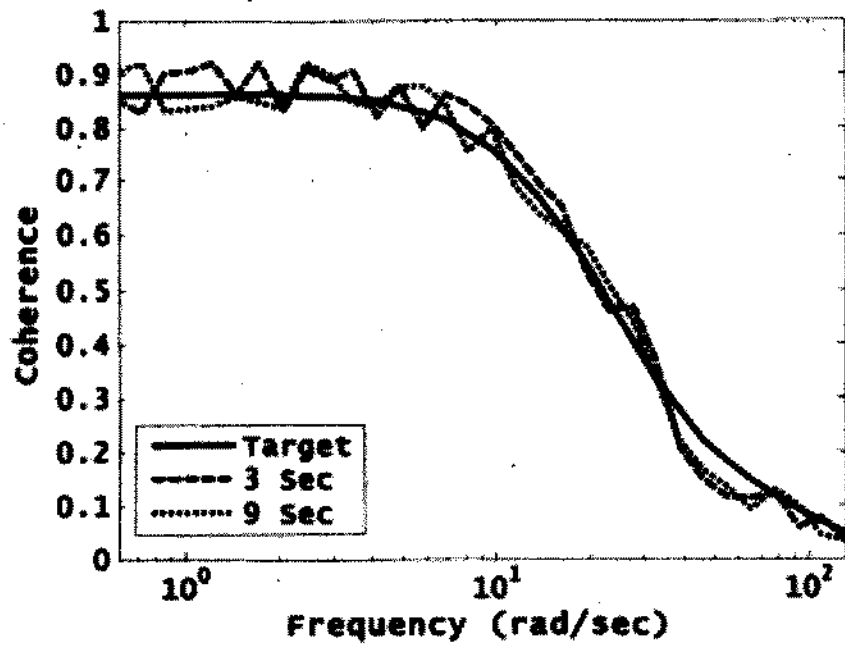


Fig. 9 Comparison of instantaneous coherences for the ensembles of accelerograms with example motion characteristics at stations 2 and 4 with the target coherence

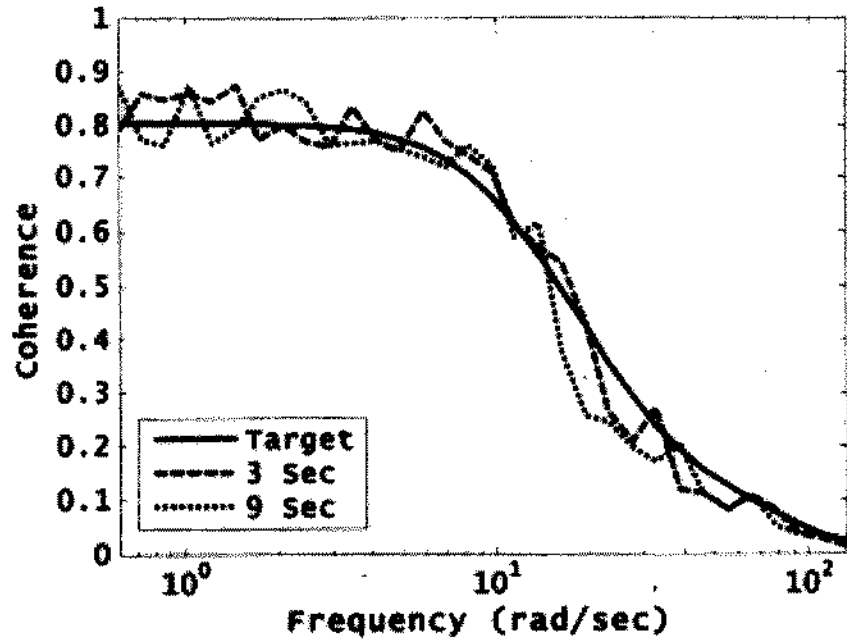


Fig. 10 Comparison of instantaneous coherences for the ensembles of accelerograms with example motion characteristics at stations 1 and 4 with the target coherence